Small angle magnetization rotation of amorphous ribbons under tensile and compressive stress

P. L. ROSSITER, T. KEANE
Department of Materials Engineering, Monash University, Clayton, Victoria 3168, Australia

Small angle magnetization rotation of Metglas 2826MB, 2605SC and 2605CO and Vitrovac 4040 ribbons under both tensile and compressive stress is investigated. It appears that there is no significant difference between the saturation magnetostriction of a ribbon when measured in tension or compression. Values determined for λ_s are 2826MB: $12.5 \pm 0.7 \times 10^{-6}$; 2605SC: $30 \pm 2 \times 10^{-6}$; 2605CO: $37 \pm 2 \times 10^{-6}$ and 4040: $10.4 \pm 0.7 \times 10^{-6}$.

1. Introduction
Application of a stress to a magnetic material will cause a rearrangement of the magnetic dipoles. This is usually called the inverse magnetostrictive or magnetomechanical effect. In a crystalline material, the action of magnetocrystalline anisotropy can result in a stress-induced change of magnetization that depends upon the nature of the stress, whether compressive or tensile, and also upon the particular direction of stress in relation to the crystal axes. Furthermore, the magnitude of the saturation magnetostriction may depend upon the level of the stress applied. This is again due to the combined action of the magnetocrystalline and magnetoelastic anisotropies and the domain configuration. This type of behaviour is reviewed by Cullity [1]. An ideally amorphous magnetic material should not exhibit either of these effects due to the absence of both magnetocrystalline and magnetoelastic anisotropies in the bulk material. However in practice these materials are prepared by splat quenching or melt spinning and often exhibit composition inhomogeneities and local short range ordering. It is thus not clear whether a real material will exhibit this ideal behaviour. Furthermore, such materials are only available in this ribbon form because of the requirements of high quench rates, and most coventional methods of determining magnetoelastic parameters with strain gauges or moving electrodes, for example, are unsuitable due to the transducer stiffness. Narita *et al.* [2] have described a novel method for determination of the saturation magnetization λ_s which is eminently suitable for such ribbons. This method, which is derived from the earlier work of Konishi *et al.* [3], is based on the measurement of small angle magnetization rotation to determine the change in the stress-induced anisotropy field. In their work a tensile stress was applied by a system of weights and results given for Metglas 2826 ($Fe_{40}Ni_{40}P_{14}B_6$) and 2605 ($Fe_{80}B_{20}$) ribbons and a ribbon of $Co_{76.7}Si_{13.3}B_{10}$.

In this paper we describe a modification of this technique which allows application of both tensile and compressive stresses. Results are given for Metglas 2826MB, 2605SC and 2605CO ribbons manufactured by Allied Chemical Company and a Vitrovac 4040 ribbon made by Vacuumschmeltze with compositions $Fe_{40}Ni_{38}Mo_4B_{18}$, $Fe_{81}B_{13.5}Si_{3.5}C_2$, $Fe_{67}Co_{18}B_{14}Si$ and $Fe_{40}Ni_{40}$ (Mo, Si, B)$_{20}$, respectively.

2. Theory
The theory and calculations relating to this technique are given in [2] and so only a brief summary will be presented here. Consider a section of amorphous ribbon placed in a magnetic field $H_\parallel$ which is directed along the ribbon axis. If the field is large enough to cause saturation, all of the moments will be aligned with the ribbon axis. If now a small amplitude a.c. field $H_\perp$ is applied perpendicular to the ribbon axis (but still in the plane of the ribbon), the moments will rotate back and forth through an angle $2\theta_{max}$ as shown schematically in Fig. 1. The angle θ will depend upon the relative magnitudes of $H_\parallel$ and $H_\perp$ and demagnetizing effects. For a transverse field of $H_\perp = H_{\perp max} \sin \omega t$, the fluctuating direction of magnetization induces a voltage e in the sense coil given by

$$e = -\tfrac{1}{2} NSM_s\omega \sin^2 \theta_{max} \sin 2\omega t \qquad (1)$$

where N is the number of turns in the sense coil and S is the cross-sectional area of the ribbon. From an energy balance Narita *et al.* [2] show that

$$\sin \theta_{max} = \frac{H_{\perp max}}{H_\parallel + H_k + H_s} \qquad (2)$$

where $H_k = 3\lambda_s\sigma/M_s$ and $H_s = M_s(N_\perp + N_\parallel)$.

In this technique the amplitude of $H_\perp$ is kept smaller than $H_\parallel$ so that $\cos \theta_{max} \simeq 1$.

From Equations 1 and 2 it is clear that a change in stress $\Delta\sigma$ produces a change in the stress anisotropy field H_k and so a change in e. However, e may be restored to its previous value by making a suitable change to the parallel field $\Delta H_\parallel$, in which case

$$\lambda_s = \frac{1}{3}\frac{\Delta H_\parallel}{\Delta \alpha} M_s \qquad (3)$$

0022–2461/86 $03.00 + .12

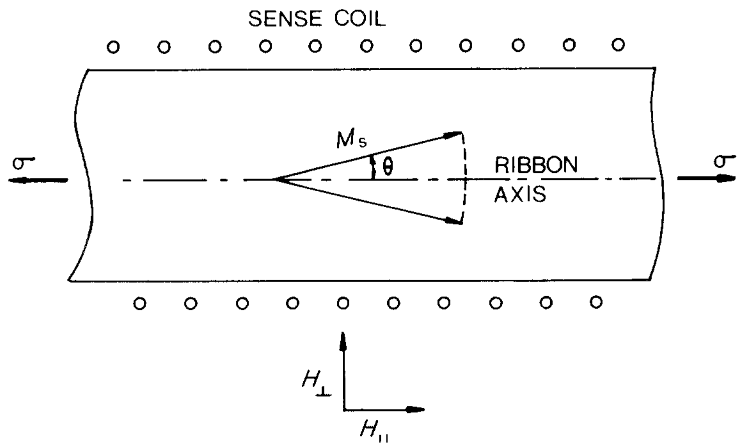

Figure 1 Schematic diagram of magnetization and field applied during measurement.

A plot of $\Delta H_{\parallel}$ against $\Delta\alpha$ (keeping e constant) should thus be linear with a slope proportional to λ_s.

3. Experimental arrangement

The parallel field $H_{\parallel}$ was applied using an electromagnet with 10 cm ϕ pole pieces spaced 13 cm apart. The a.c. perpendicular field $H_{\perp}$ was supplied by a pair of coils each 2 cm ϕ and 2.5 cm long wound with 100 turns of copper wire. The sense coil was 2.5 cm in length and had an internal diameter of 0.8 cm and was wound with 1000 turns of copper wire. The coils were held in an aluminium frame to maintain their orthogonal alignment. Each ribbon specimen 5 cm long and 0.5 cm wide was bonded to a brass substrate of dimensions 11 cm × 0.7 cm × 0.2 cm with a 2 h cure–time epoxy resin. Stresses were applied with a simple four-point bend apparatus constructed from aluminium and which consists of four support rods rising from a base which sits on the frame of the electromagnet whilst positioning the middle of the specimen and sense coil at the saddle point of the field. The two inner rods hold up roller supports for the specimen substrate, whereas the outer rods have a screw mechanism for adjusting the bending moment. Hence, if the substrate is placed with the specimen uppermost, the specimen will be put into tension as the screws are advanced, and when the substrate has the specimen on the lower side, the stress will be compressive. As the ribbons were much thinner than the substrates (~ 50 μm compared to 0.2 cm) the strain in each ribbon was assumed to be uniform and uniaxial. The bending apparatus was calibrated by bonding an electrical resistance strain gauge to one of the specimens and measuring strain as a function of screw advancement. This calibration was quite linear and is shown in Fig. 2.

A block diagram of the equipment used to drive and monitor the system is shown in Fig. 3. The sense coil

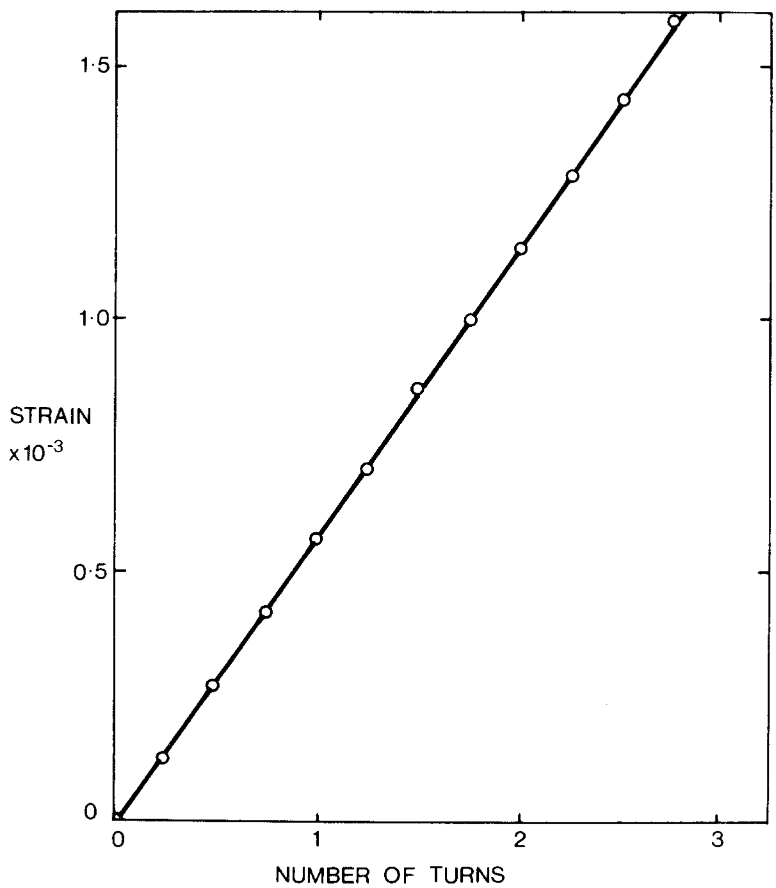

Figure 2 Calibration curve for strain produced in four-point bend apparatus.

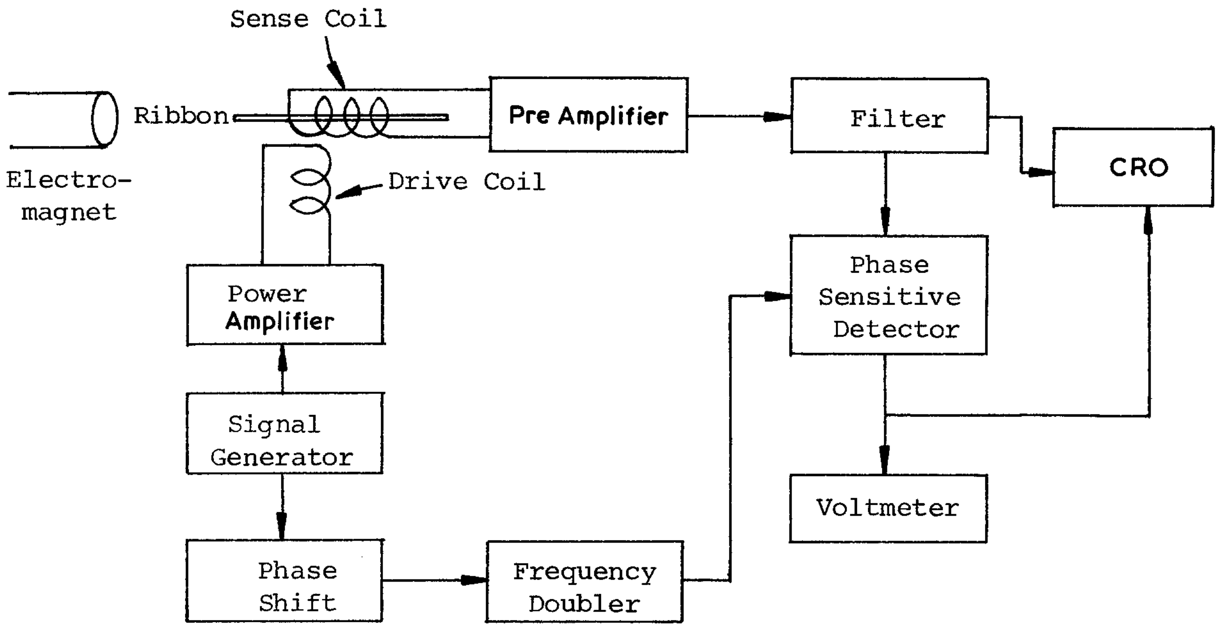

Figure 3 Block diagram of electronic apparatus.

output was preamplified and passed through a filter tuned to twice the $H_{\perp}$ frequency, as required by Equation 1. This filter had a bandwidth of 1 Hz. The signal was then detected with a phase sensitive detector and voltmeter.

4. Results and discussion

The initial parallel field was chosen to exceed that required to produce saturation of the ribbons (typically $80\,\mathrm{A\,m^{-1}}$) and in this study was set at $2.7 \times 10^4\,\mathrm{A\,m^{-1}}$. It was monitored with a conventional Hall

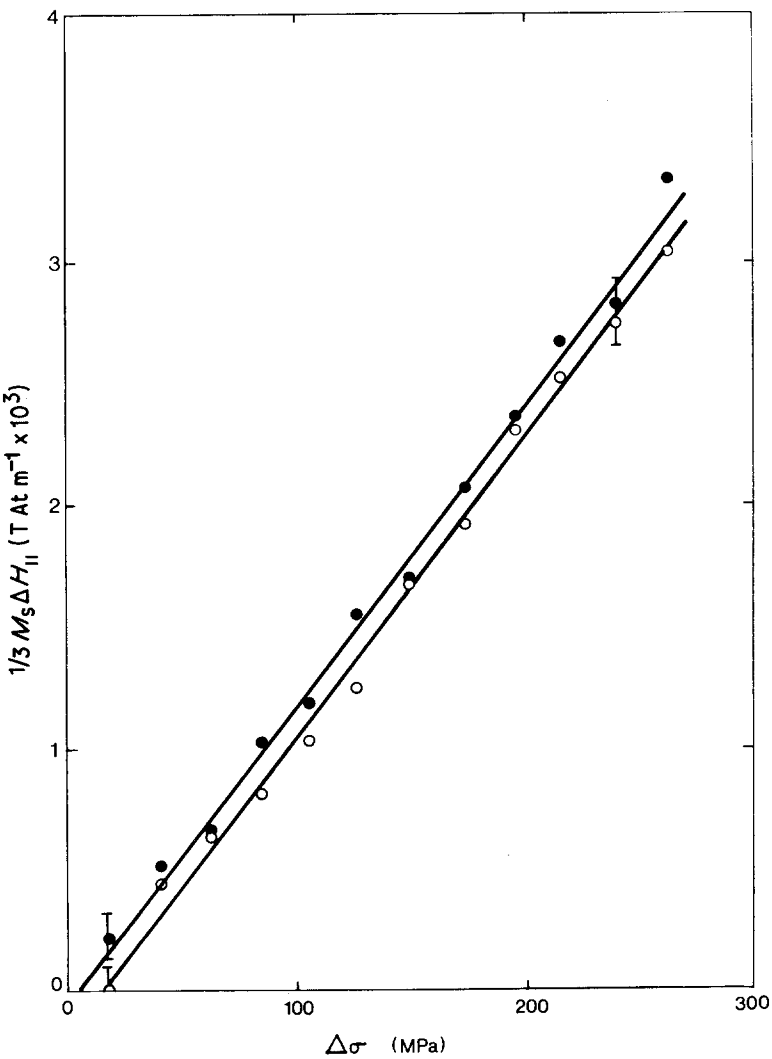

Figure 4 Dependence of $\frac{1}{3}M_s\Delta H_{\parallel}$ on $\Delta\sigma$ for 2826MB ribbon. (○) compression; (●) tension.

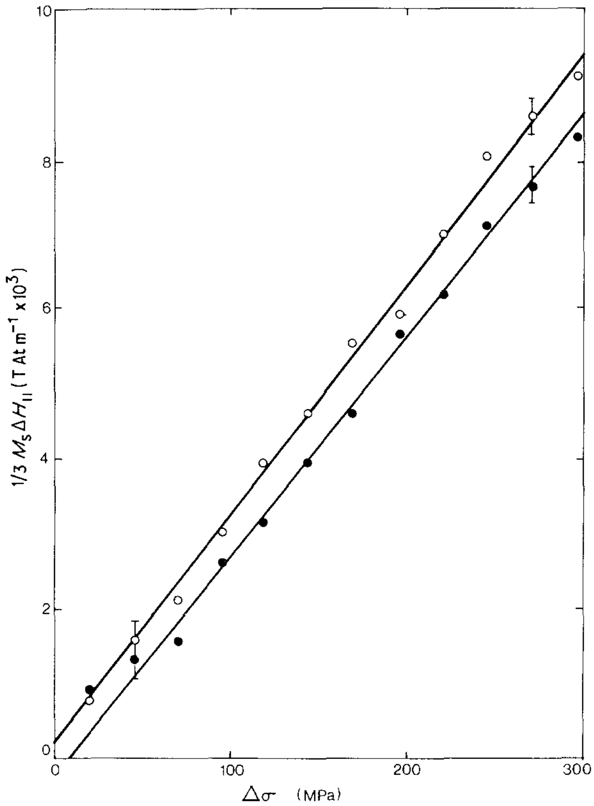

Figure 5 Dependence of $\frac{1}{3}M_s\Delta H_{\|}$ on $\Delta\alpha$ for 2605SC ribbon. Symbols as for Fig. 4.

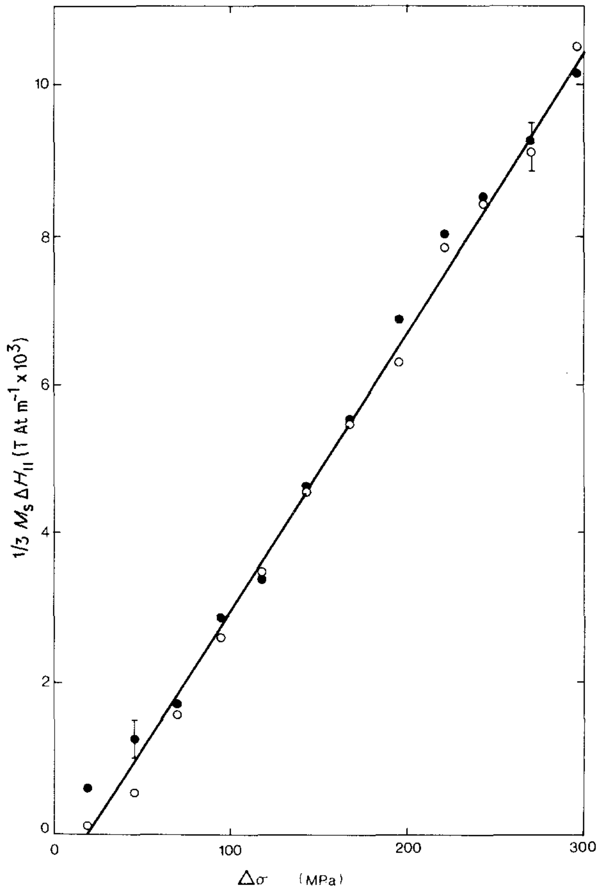

Figure 6 Dependence of $\frac{1}{3}M_s\Delta H_{\|}$ on $\Delta\sigma$ for 2605CO ribbon. Symbols as for Fig. 4.

probe. The peak value of $H_\perp$ was $1.8 \times 10^3\,\mathrm{A\,m^{-1}}$ giving a maximum magnetization rotation angle of about 4° satisfying the condition $\cos\theta_{max} \simeq 1$. The frequency of $H_\perp$ was set in the range 60 to 90 Hz so as to avoid interference from the 50 Hz power mains.

The data obtained from the four ribbons investigated are given in the plots of $\frac{1}{3}M_s\Delta H_{\|}$ against $\Delta\sigma$ shown in Figs 4 to 7. The stress was determined from the known strain and Young's modulus E. Values of E and B_s were taken from the literature and are shown in Table I. The values of E for the 2605SC and 2605CO ribbons were not available and so were taken as being equal to that of Metglas 2605 ($Fe_{80}B_{20}$). Considering the variation of E with composition of similar amorphous alloys [4], it is reasonable to assume that the value for 2605SC should not vary from that of 2605 by more than 5%. The value for 2605CO may however be less accurate. Due to the nature of the apparatus, the zero of stress was somewhat arbitrary and so the tension and compression curves may be displaced along the stress axis.

The saturation magnetostrictions of the four alloys were determined from the gradients of the above mentioned plots and are quoted in Table II with error ranges calculated from the maximum and minimum gradients within the error bars on the plots. Hence the inaccuracies associated with the constants E and M_s are not accounted for here, although these quantities are conventionally measurable to within 2%. Also shown in Table II are corresponding values quoted in the literature.

TABLE I Published values of E and M_s used to determine λ_s

Alloy	E(GPa)	[Reference]	$M_s(T)$	[Reference]
2826MB	150	[5]	0.88	[8]
2605	169	[4]		
2605SC	169		1.57	[7]
2605CO	169		1.75	[7]
4040	150	[6]	0.8	[6]

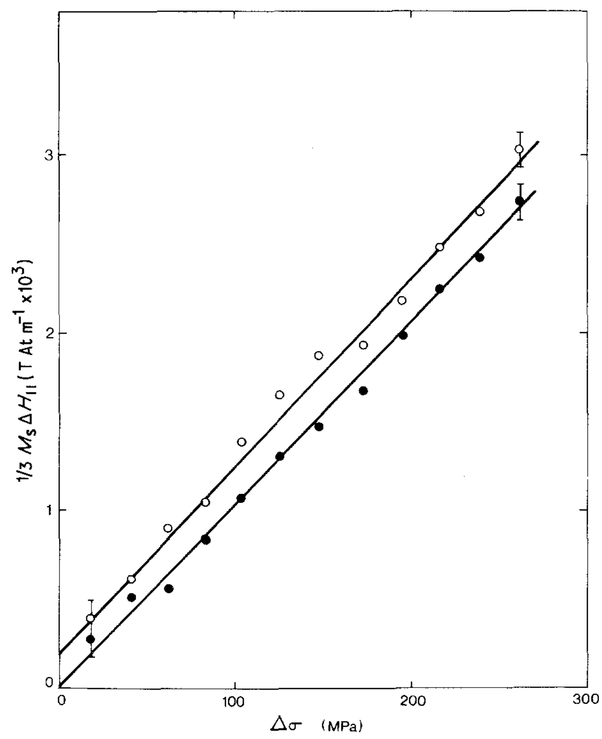

Figure 7 Dependence of $\frac{1}{3}M_s\Delta H_{\|}$ on $\Delta\sigma$ for 4040 ribbon. Symbols as for Fig. 4.

TABLE II Calculated values of λ_s compared with those reported elsewhere

Alloy	Compression	$\lambda_s \times 10^6$ Tension	Reported	[Reference]
2826MB	12.5 ± 0.7	12.2 ± 0.7	12	[7]
2605SC	30 ± 2	30 ± 2	30	[7]
2605CO	37 ± 2	37 ± 2	35	[7]
4040	10.4 ± 0.7	10.2 ± 0.7	8	[6]

From these results it appears that there is no significant difference between the saturation magnetostrictions of the amorphous ribbons when measured in tension or compression. The values obtained here are seen to be slightly higher than those reported elsewhere. This may be a consequence of the method of measurement as the same trend was noticed in the original work with the technique by Narita *et al.* [2]. It might also reflect the errors associated with transducer stiffness in the other works cited.

The scatter in the experimental data could be reduced by increasing the frequency of the a.c. drive field $H_\perp$ (provided that the skin depth does not become less than the ribbon thickness) and/or employing a more sensitive voltmeter than the single moving coil instrument used in this study.

References

1. B. D. CULLITY, in "Introduction to Magnetic Materials" (Addison-Wesley, Reading, Massachusetts, 1972) p. 248.
2. K. NARITA, J. YAMASAKI and H. FUKUNAGA, *IEEE Trans. Mag.* **Mag-16** (1980) 435.
3. S. KONISHI, S. SUGATANI and Y. SAKURAI, *ibid.* **5** (1969) 14.
4. L. A. DAVIS, in "Rapidly Quenched Metals" edited by N. J. Grant and B. C. Giessen (Massachusetts Institute of Technology, Massachusetts, 1976) p. 369.
5. E. TOROK and G. HAUSCH, in "Rapidly Quenched Materials III" Vol. 2 (The Metals Society, London, 1978) p. 107.
6. Vacuumschmelze, Vitrovac 4040 Preliminary Data Sheet M5509a-02 (1981).
7. Allied Corporation, Metglas Alloys Preliminary Information Booklet ISM-10/81 (1981).
8. B. D. CULLITY, *ibid.*, p. 278.

Received 30 September
and accepted 18 November 1985